2015

Somatic chromosomal translocation between Ewsr1 and Fli1 loci leads to dilated cardiomyopathy in a mouse model

Miwa Tanaka
Japanese Foundation for Cancer Research

Shuichi Yamaguchi
Japanese Foundation for Cancer Research

Yukari Yamazaki
Japanese Foundation for Cancer Research

Hideyuki Kinoshita
Kyoto University Graduate School of Medicine

Koichiro Kuwahara
Kyoto University Graduate School of Medicine

See next page for additional authors

SCIENTIFIC REPORTS

OPEN

SUBJECT AREAS:
GENE REGULATION
CARDIOMYOPATHIES
DNA RECOMBINATION
CYTOGENETICS

Received
28 August 2014

Accepted
12 December 2014

Published
16 January 2015

Correspondence and requests for materials should be addressed to T.N. (takuro-ind@umin.net)

Somatic chromosomal translocation between *Ewsr1* and *Fli1* loci leads to dilated cardiomyopathy in a mouse model

Miwa Tanaka[1], Shuichi Yamaguchi[1], Yukari Yamazaki[1], Hideyuki Kinoshita[2], Koichiro Kuwahara[2], Kazuwa Nakao[2], Patrick Y. Jay[3], Tetsuo Noda[4] & Takuro Nakamura[1]

[1]Division of Carcinogenesis, The Cancer Institute, Japanese Foundation for Cancer Research, 3-8-31 Ariake, Koto-ku, Tokyo 135-8550, Japan, [2]Department of Cardiovascular Medicine, Kyoto University Graduate School of Medicine, 54 Kawaracho Shogoin, Sakyo-ku, Kyoto 606-8507, Japan, [3]Departments of Pediatrics and Genetics, Washington University School of Medicine, 660 S Euclid Avenue, St. Louis, MO 63110, U.S.A, [4]Division of Cell Biology, The Cancer Institute, Japanese Foundation for Cancer Research, 3-8-31 Ariake, Koto-ku, Tokyo 135-8550, Japan.

A mouse model that recapitulates the human Ewing's sarcoma-specific chromosomal translocation was generated utilizing the *Cre/lox*P-mediated recombination technique. A cross between *Ewsr1-lox*P and *Fli1-lox*P mice and expression of ubiquitous Cre recombinase induced a specific translocation between *Ewsr1* and *Fli1* loci in systemic organs of both adult mice and embryos. As a result *Ewsr1-Fli1* fusion transcripts were expressed, suggesting a functional Ews-Fli1 protein might be synthesized *in vivo*. However, by two years of age, none of the *Ewsr1*-loxP/*Fli1*-loxP/CAG-Cre (EFCC) mice developed any malignancies, including Ewing-like small round cell sarcoma. Unexpectedly, all the EFCC mice suffered from dilated cardiomyopathy and died of chronic cardiac failure. Genetic recombination between *Ewsr1* and *Fli1* was confirmed in the myocardial tissue and apoptotic cell death of cardiac myocytes was observed at significantly higher frequency in EFCC mice. Moreover, expression of *Ews-Fli1* in the cultured cardiac myocytes induced apoptosis. Collectively, these results indicated that ectopic expression of the *Ews-Fli1* oncogene stimulated apoptotic signals, and suggested an important relationship between oncogenic signals and cellular context in the cell-of-origin of Ewing's sarcoma.

Chromosomal translocation is a common feature of malignant neoplasms[1]. There is growing evidence that tumor-specific translocations and inversions commonly occur among hematopoietic, mesenchymal and epithelial tumors. An increasing number of gene fusions resulting from translocation have been observed as novel technological tools have been applied. Tumor-associated chromosomal translocations include two major molecular mechanisms. One is an oncogene juxtaposition to the enhancing elements of immunoglobulin or T-cell receptor associated with lymphoid neoplasms. As a result of the juxtaposition, constitutive expression of oncogenes such as *c-MYC, BCL2* or *CCND1* induces abnormal cellular functions, including cell cycle progression and apoptosis suppression[1]. Another important outcome of translocation in cancer is gene fusion or formation of chimeric genes. Two major functional aberrations of fusion gene products are constitutive activation of signal transduction and dysregulation of transcription. Most oncogenic gene fusions in human bone and soft tissue sarcomas belong to the latter group, and there is a specific relationship between tumor types and each gene fusion[2].

To clarify the functional roles of sarcoma-specific chromosomal translocations and gene fusions, it would be ideal to induce chromosomal translocation in animal models *in vivo*. In contrast to transgenic expression of fusion genes, translocation-mediated gene fusion recapitulates gene expression levels equivalent to, and splice variants similar to those in human tumors. Inducible, site-specific chromosomal translocation has been achieved using Cre-*lox*P-mediated recombination in murine ES cells. Using this strategy, translocations between c-myc and immunoglobulin heavy chain loci, and between *Dek* and *Can* loci were successfully induced, though the efficiencies were not very high[3,4]. Indeed, a mouse model of Cre-*lox*P-mediated *in vivo* gene fusion between *Mll* and *Af9* developed acute myeloid leukemia[5]. However, it is not known whether solid tumor-related translocation *in vivo* can induce malignancies of the anticipated phenotypes.

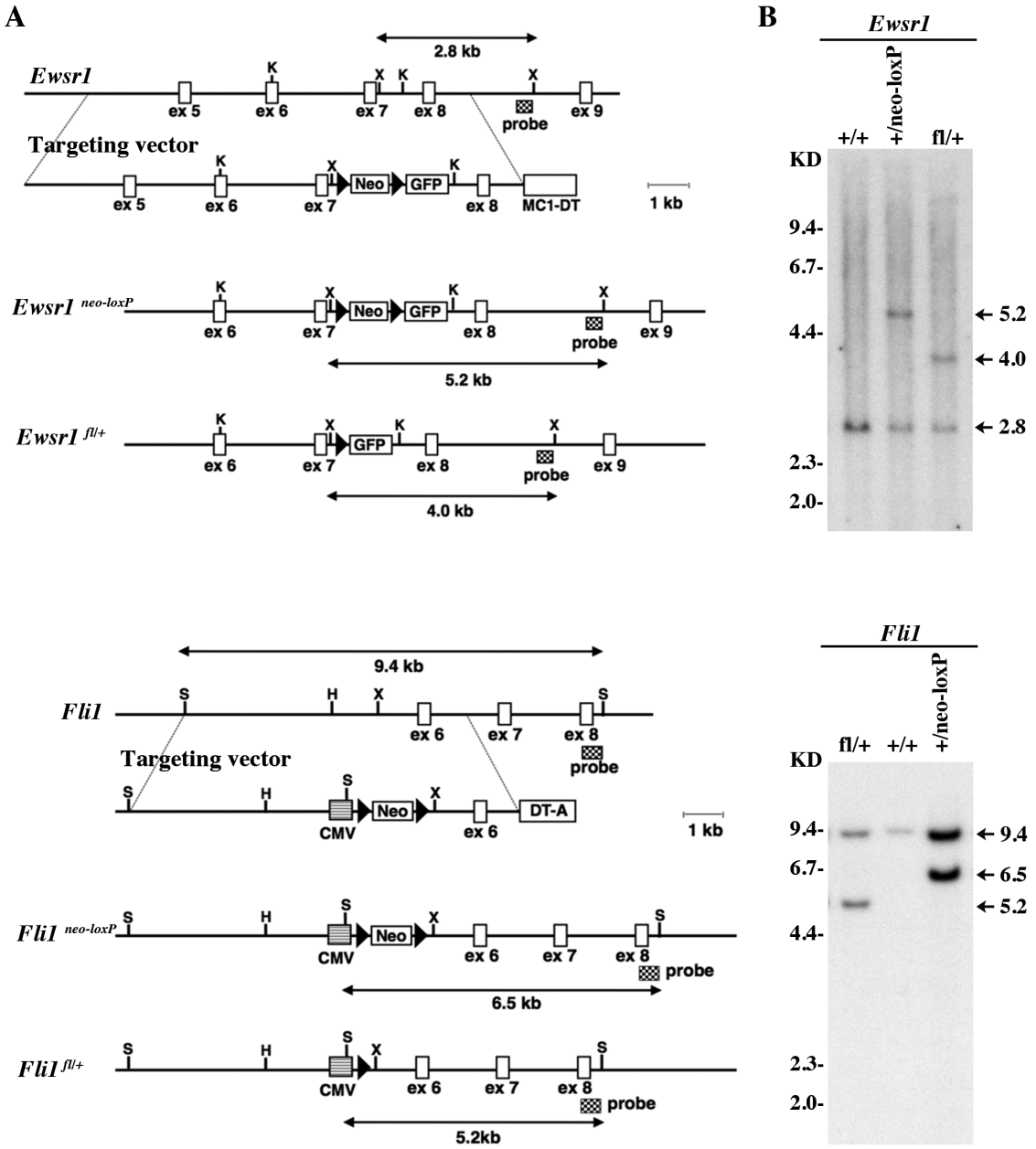

Figure 1 | Gene targeting for the *Ewsr1-Fli1* translocation model. (A) Physical maps of targeting alleles for *Ewsr1* (top) and *Fli1* (bottom) loci. Closed triangles indicate the *lox*P sequence. K: *Kpn*I, X: *Xba*I, S: *Sac*I, H: *Hin*dIII. (B) Southern blot analysis of ES cells. A 5.2 kb *Neo*-positive band and a 4.0 kb *Neo*-deleted band indicate homologous recombination of the *Ewsr1* locus as shown by *Xba*I digestion (top). A 6.5 kb *Neo*-positive band and a 5.2 kb *Neo*-deleted bands for the *Fli1* locus are shown by *Sac*I digestion (bottom). Rearranged bands are indicated by arrows.

The ETS family of transcription factors includes FLI1 and ERG. They are major fusion partners for the *EWSR1* gene in human Ewing's sarcoma[6,7]. EWS-FLI1 and EWS-ERG function as oncogenic transcription factors that dysregulate their downstream targets such as *NKX2-2*, *NR0B1* and *EZH2*[8]. It is, however, difficult to generate a good animal model by introduction of *EWS-FLI1* or *EWS-ERG* into ES cells or mouse eggs[8]. Moreover, conditional *EWS-FLI1* expression in hematopoietic cells induced myeloid and erythroid leukemia in mice[9]. Thus, it might be necessary to activate multiple target genes without activating pro-apoptosis signals for tumorigenic activity of EWS-ETS. We therefore hypothesized that EWS-ETS translocation is achieved by chance in human somatic cells of appropriate lineages and differentiation status, and such *in vivo* translocation could properly induce Ewing's sarcoma.

In an effort to induce Ewing's sarcoma in a mouse model, we have succeeded in promoting *in vivo* Cre-*lox*P-mediated translocation between *Ewsr1* and *Fli1* loci on chromosomes 11 and 9, respectively. Although the *Ewsr1-Fli1* fusion was confirmed at both DNA and RNA levels, no neoplastic lesion was induced in the model. Unexpectedly, the mice with systemic translocation developed dilated cardiomyopathy due to degeneration and apoptotic cell death of cardiac myocytes. The result indicates that ectopic chromosomal translocation and gene fusion activates apoptotic signals, resulting in degenerative cardiac disease.

Results

Generation of a mouse model for somatic chromosomal translocation between *Ewsr1* and *Fli1*. To induce locus-specific chromosomal translocation, *lox*P sequences were introduced into *Ewsr1* intron 7 on mouse chromosome 11 and *Fli1* intron 5 on chromosome 9 (Fig. 1A), since chromosomal breakpoints in human Ewing's sarcoma are most frequently observed in these loci[10]. Successful

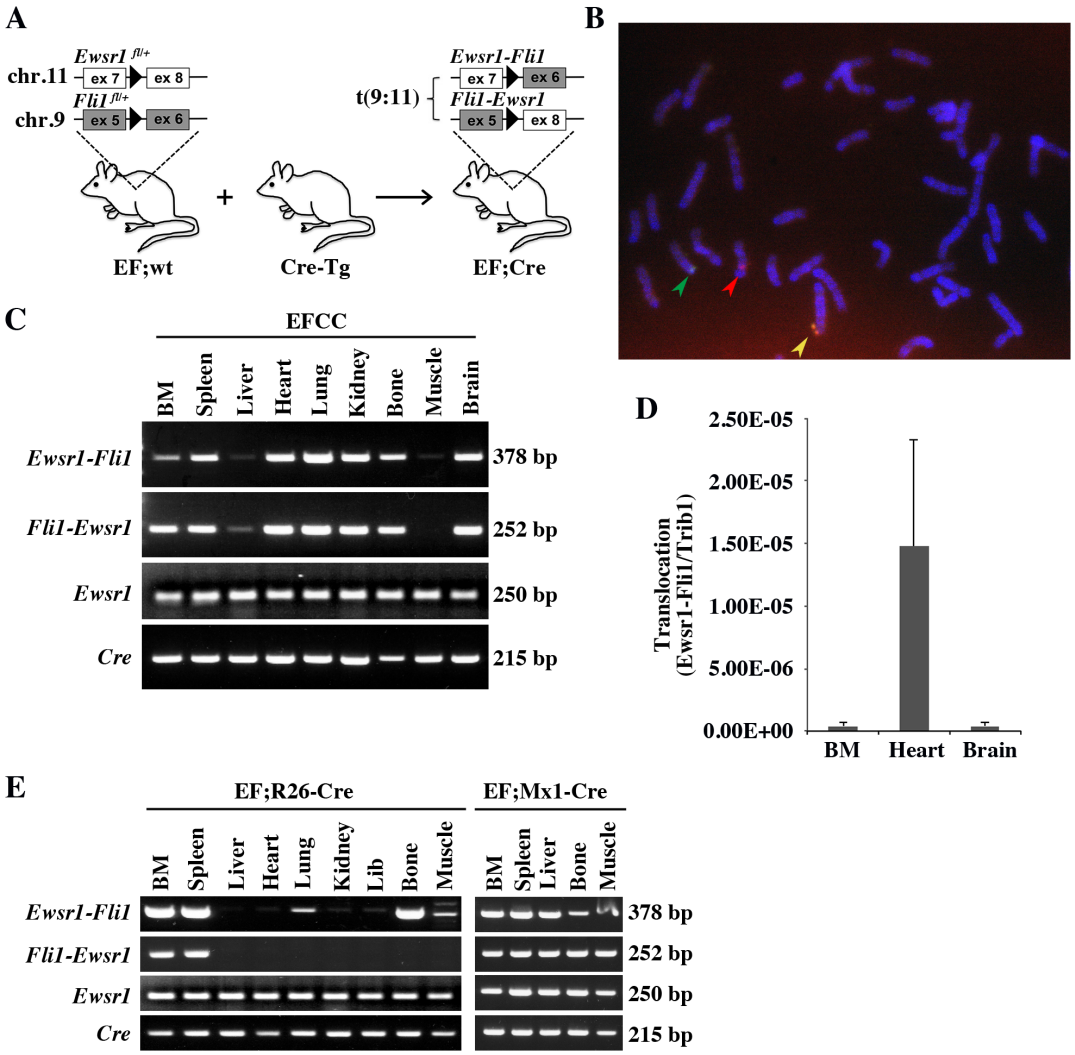

Figure 2 | Somatic chromosomal translocation between mouse chromosomes 9 and 11. (A) A schematic diagram of the *Cre*-mediated translocation model. EF;wt, *Ewsr1*$^{fl/+}$:*Fli1*$^{fl/+}$:wild-type. Cre-Tg, *Cre* transgenic. EF;Cre, *Ewsr1*$^{fl/+}$:*Fli1*$^{fl/+}$: *Cre* transgenic. Illustration of mice was drawn using Microsoft PowerPoint 2011 and then converted to tif format using Adobe Photoshop CS5. (B) Metaphase FISH shows t(9;11) translocation at *Ewsr1* and *Fli1* loci. The green fluorescence of 64E17 shows *Ewsr1* on chromosome 11 and the red fluorescence of 218O21 shows *Fli1* on chromosome 9. The yellow signal indicates translocation between two loci on *der9*. (C) The reciprocal t(9;11) translocation was shown in systemic organs of the EFCC mouse detected as *Ewsr1-Fli1* and *Fli1-Ewsr1* PCR products. *Ewsr1* amplification is shown as a loading control. (D) Estimated frequencies of translocation in bone marrow (BM), heart and brain calculated from the result of quantitative genomic PCR data in three independent mouse samples. (E) The reciprocal t(9;11) translocation in the organs of *Rosa26-CreER* and *Mx1-Cre* background detected by nested genomic PCR. Gel image shown is cropped and representative of gels run under the same experimental conditions.

knock-in of *lox*P sequences mediated by homologous recombination was confirmed for both loci in independent ES cells by Southern blotting (Fig. 1B). Both *Ewsr1*$^{fl/+}$ and *Fli1*$^{fl/+}$ mice appeared normal and healthy at birth. Germline transmission of the targeted alleles was confirmed. *Ewsr1*$^{fl/+}$ and *Fli1*$^{fl/+}$ mice were crossed to obtain mice having both mutations.

Genomic chromosomal translocation between chromosomes 9 and 11 in the *Ewsr1*$^{fl/+}$:*Fli1*$^{fl/+}$:*CAG-Cre* (EFCC) mice. The *Ewsr1*$^{fl/+}$ and *Fli1*$^{fl/+}$ mice were further crossed with *CAG-Cre*, *Mx1-Cre* or *Rosa26-CreER* mice to induce somatic chromosomal translocation between chromosomes 9 and 11 (Fig. 2A). Dual color fluorescence *in situ* hybridization (FISH) analysis of embryonic fibroblasts derived from the EFCC mice showed juxtaposition of the signal on *der9* of BAC clone RPCI-23 64E17 from chromosome 11 and that of 218O31 from chromosome 9 (Fig. 2B). Reciprocal genomic translocations in systemic organs were examined by genomic PCR using *Ewsr1*- and *Fli1*-specific primers, and both *Ewsr1-Fli1* and *Fli1-Ewsr1* translocations were detected in tail skin of all the mice examined (n = 30). The translocations in systemic organs were examined in three mice, and both *Ewsr1-Fli1* and *Fli1-Ewsr1* translocations were detected in all the organs examined (Fig. 2C). The results indicated that *lox*P-mediated recombination was effective at inducing somatic translocation by ubiquitous *Cre* recombinase expression. The frequencies of the chromosomal translocations were 1.5×10^{-5} at the highest in heart and 1×10^{-6} in bone marrow as estimated by quantitative genomic PCR comparing *Ewsr1-Fli1* and *Trib1* signals (Fig. 2D). The estimated translocation frequencies in the model are higher than those observed in ES cells described in the previous report[3]. When *Cre* recombinase was inducibly expressed by tamoxifen or polyIpolyC administration in a *Rosa26-CreER* or *Mx1-Cre* background, respectively, both *Ewsr1-Fli1* and *Fli1-Ewsr1* translocations were observed (four mice each) (Fig. 2e). However, the translocations

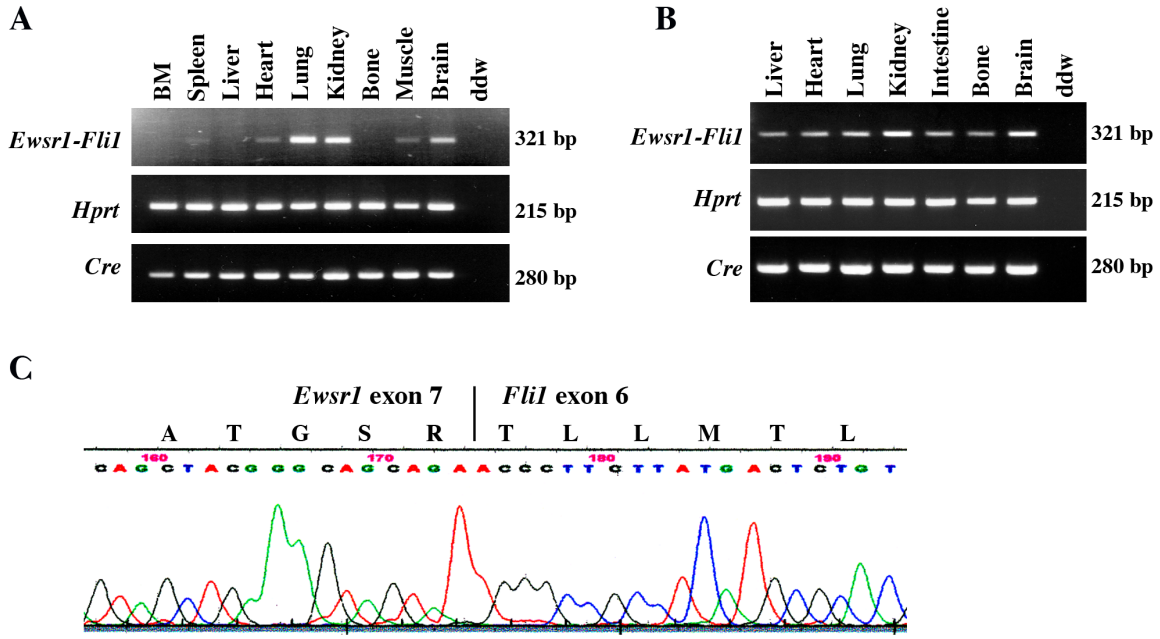

Figure 3 | ***Ewsr1* is fused in-frame to *Fli1*.** (A, B) RT-PCR to detect *Ews-Fli1* fusion transcripts in adult (A) and embryonic tissues (B). Data are representatives of three independent experiments with similar results. (C) Sequence analysis of the RT-PCR product using heart cDNA shows the in-frame fusion between *Ewsr1* exon 7 and *Fli1* exon 6. Deduced amino acid sequences are indicated on the nucleotide sequences.

were detected only by nested PCR in limited organs, indicating that recombination was less frequent in these *Cre* transgenes. In addition, inducible expression of *Cre* upon in the *Mx1-Cre* background resulted in translocations being limited to hematopoietic tissues.

Detection of chimeric *Ewsr1-Fli1* fusion transcripts in EFCC mice. To confirm that gene fusion between *Ewsr1* and *Fli1* was accompanied by the anticipated transcription, RT-PCR was performed using RNA samples obtained from systemic organs of both adult and embryonic mice (three mice each) (Fig. 3A, 3B). The *Ewsr1-Fli1* fusion was detected in all the embryonic organs examined, and the expression of the fusion gene was decreased in bone and liver of the adult mice. Diminished *Ewsr1-Fli1* expression in adult bone and liver might be related to decreased proliferative activity of osteochondrogenic tissues and disappearance of embryonic hematopoietic cells, respectively. No reciprocal *Fli1-Ewsr1* fusion transcript was detected in any of the organs examined (data not shown). The cDNA sequence of the *Ewsr1-Fli1* fusion transcript was analyzed by sequencing, and in-frame fusion between *Ewsr1* exon 7 and *Fli1* exon 6 was confirmed (Fig. 3C). It is expected that the fusion product included both the EWS Q-rich repeats and the FLI1 ETS DNA binding domain[11]. Thus, the data strongly suggested that a functional EWS-FLI1 protein was produced by somatic chromosomal translocation in the model.

EFCC mice died of chronic cardiac failure due to dilated cardiomyopathy. No malignant neoplasms, including Ewing's sarcoma-like lesions, were observed in EFCC mice (n = 30) for a two year period after birth. Neither sarcomas nor benign neoplasms were detect by careful examination of mice irrespective of age. Instead, most of the EFCC mice showed growth retardation and decreased motility. All the EFCC mice died by 100 weeks of age with a mean survival time of only 40 weeks (Fig. 4A). The diseased mice were carefully examined at autopsy and they showed extensive dilatation of heart (Fig. 4B). The heart weight/body weight ratio as well as heart weight itself of EFCC mice was significantly greater than that of control mice from 31 to 42 weeks (Fig 4C, Table 1). Mice of the age were selected since the severity of cardiac lesions was significantly varied in younger EFCC mice. The pathological examination further revealed the cardiac lesions and subsequent systemic congestive changes. The hearts of EFCC mice showed extensive dilatation of both the ventricles and thin ventricular wall without any signs of cardiac hypertrophy (Fig 4D). The earlier the mice became sick, the more severe the cardiac lesions were. High power views of cardiac sections indicated a disorganized arrangement of myocardial fibers with increased collagen fibers between the muscle bundles. The subendocardial area was severely affected and leukocytic infiltration was sometimes present. There was severe chronic congestion in systemic organs such as lung, liver or spleen accompanied by ischemic necrosis around the central vein of the liver (Fig. 4E).

Consistent with the pathological findings, echocardiographic analysis revealed reduced wall thickness, significant fractional shortening and decreased ejection fraction in EFCC mice (Fig. 5, Table 2). In contrast, there was no significant difference in blood pressure, heart rate or diastolic dimension between EFCC and wild-type mice (Table 2). Collectively, these findings are consistent with those of dilated cardiomyopathy.

***Ewsr1-Fli1* translocation and *Ewsr1-Fli1* expression induced myocardial damage.** To obtain insights into the mechanisms of dilated cardiomyopathy in EFCC mice, the cardiac lesion was further investigated. Laser microdissection followed by genomic PCR to detect the *Ewsr1-Fli1* translocation was carried out (Fig. 6A). *Ewsr1-Fli1* was abundantly observed in the outer area of the ventricular wall, however, no signal was detected in the subendocardial area where the myocardial damage was more severe (Fig. 6A, 1 and 3). Severer damages in the subendocardial area were observed in most of mice, though the reason for such uneven distribution of cardiac lesions was unclear. The results suggested degeneration of cardiac myocytes with translocation and perhaps gradual loss due to the pathologic effects of *Ewsr1-Fli1* expression. Indeed, a TUNEL assay using the cardiac sections showed significantly increased apoptosis in EFCC mice compared to wild-type (Fig. 6B).

The toxic effect of *Ewsr1-Fli1* was directly evaluated by its exogenous expression in cultured cardiac myocytes. The murine neonatal cardiac myocytes were infected with *Ewsr1-Fli1*-lentivirus and the frequencies of apoptosis were evaluated (Fig. 6C). The TUNEL assay

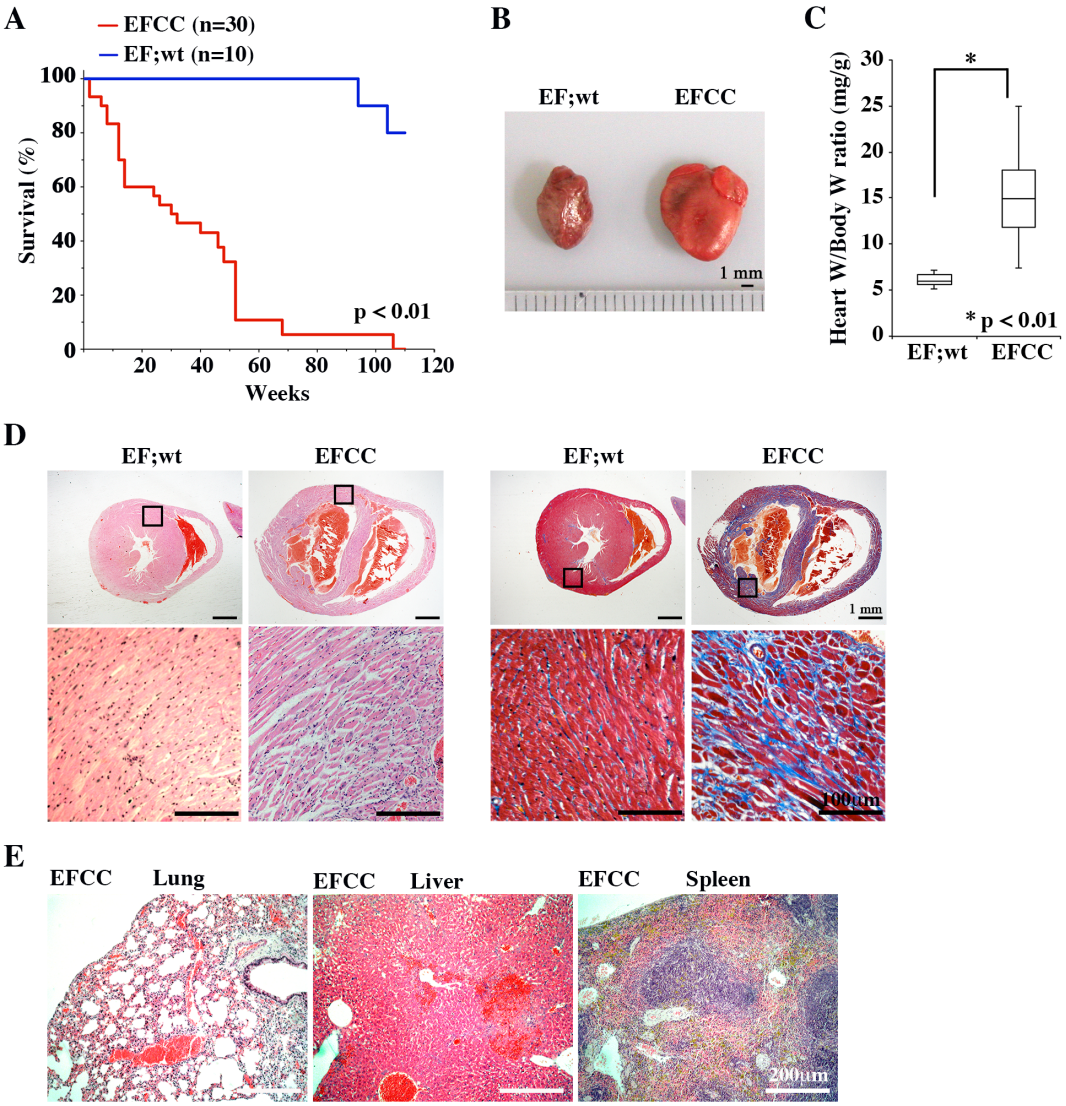

Figure 4 | EFCC mice died of chronic cardiac failure. (A) Kaplan-Meier survival curve. Statistical significance was evaluated by the log-rank test. (B) Cardiac enlargement in the EFCC mouse (right) compared to EF;wild-type (left). (C) Box plot of the heart weight/body weight ratios for EF;wild-type (n = 6) and EFCC mice (n = 6). (D) Extensive ventricular dilatation of the heart in the EFCC mouse without myocardial hypertrophy (top). High power view of myocardium with H&E (middle) and Masson's trichrome staining (bottom). Extensive fibrosis is indicated as blue staining in the EFCC heart. (E) Chronic congestion of systemic organs in EFCC mice including lung, liver and spleen. Note necrotic changes around the central vein of liver.

showed that apoptosis of cardiac myocytes was significantly increased when *Ewsr1-Fli1* was expressed in the cardiac myocytes. The Annexin V/PI flow cytometry analysis showed increases of both early and late apoptosis as well as necrosis in cardiac myocytes by *Ewsr1-Fli1* expression (Fig. 6C). These results indicated that *Ewsr1-Fli1* induced cellular apoptosis in the cardiac tissue, resulting in cellular damage and eventual dilated cardiomyopathy. In addition, *Ewsr1-Fli1* expression in human cardiac fibroblasts induced increased expression of *COL1A1* (Fig. 6D), suggesting that *Ewsr1-Fli1* may also play some role in cardiac fibrosis.

A previous study indicated that the high level of expression of Cre recombinase itself showed cardiac toxicity[12]. The expression level of the Cre protein in the hearts of the EFCC mouse was therefore compared with high-expressing *Cre* transgenic mice (Fig. 6E). *Cre* expression of EFCC mice was comparable to the low *Cre* transgenic mice that did not show cardiac lesions. The results indicated that the cardiac lesion was caused not by *Cre* expression but by *Ewsr1-Fli1*.

Discussion

Cre/*lox*P-mediated chromosomal translocations in mouse models have been reported[5,13,14]. In those studies *lox*P sites were inserted into the introns of *Mll* or *Af9* genes, and the mice carrying the mutations were crossed to place *lox*P sites in both genes. Both ubiquitous and hematopoietic-specific expression of Cre recombinase induced *in vivo* chromosomal translocation and the fusion of *Mll* and *Af9*, resulting in leukemia development. In contrast, leukemia was not observed in the mice bearing chromosomal translocation between *AML1* and *ETO in vivo* using a similar protocol[15].

In the present study, *Ewsr1-Fli1* fusion was successfully induced in various organs. Ewing's sarcoma, however, did not develop in the mice, suggesting that the cell-of-origin of Ewing's sarcoma might constitute a rare cellular population unlike hematopoietic neoplasms. Supporting this idea, we have recently succeeded in developing Ewing's sarcoma-like small round cell tumors by introducing *Ews-Fli1* or *Ews-Erg* into eSZ cells that are enriched in embryonic chondrogenic progenitors[16]. Therefore, when chromosomal translocation between *Ewsr1* and *Fli1* is efficiently induced in eSZ cells, Ewing's sarcoma can develop in a certain cohort using the current translocation model. It is likely that ubiquitous *Cre* expression affects most cell lineages both in developing and adult mouse tissues including the true cell-of-origin of Ewing's sarcoma. However, the low frequency of chromosomal recombination could

Table 1 | Heart and body weight of EF;wt and EFCC mice

EF;wt			
Weeks	HW (mg)	BW (g)	HW (mg)/BW (g)
31	180	25.25	7.13
36	140	27.50	5.09
36	140	25.38	5.52
38	210	34.58	6.07
38	180	26.15	6.88
40	150	25.66	5.85
EFCC			
Weeks	HW (mg)	BW (g)	HW (mg)/BW (g)
30	360	19.63	18.34
35	640	25.47	25.12
36	320	25.66	12.47
36	260	22.49	11.56
40	410	23.66	17.33
42	120	16.22	7.40

not induce detectable translocations in such a rare cell type. Perhaps eSZ cell-specific *Cre* expression may enable the induction of Ewing's sarcoma by somatic *Ewsr1* and *Fli1* translocation, and efficient *Cre* expression in the specific spatiotemporal manner in the eSZ cell may be achieved using the promoter/enhancer elements of *Gdf5* or *Erg* genes[17,18].

Expression of *Ews-Fli1* in the majority of primary cells induced cellular apoptosis or senescence[19–21]. Activation of the *Casp3* promoter by EWS-FLI1 was reported, and the activation of caspase 3-dependent signals may be responsible for apoptotic processes in mouse embryonic fibroblasts (MEFs) with ectopic *Ews-Fli1* expression[21]. Indeed, *Ews-Fli1* expression in cardiac myocytes induced apoptotic cell death, though activation of caspase 3 was not detected in cardiac myocytes unlike in MEFs (data not shown). Thus, the low capacity for cardiac myocyte regeneration after birth could not support cardiac homeostasis. This limitation, therefore, could result in gradual but irreversible cardiac damage. In support of this idea, the *Ews-Fli1* fusion was not detected in the severely degenerated area but remained in relatively normal parts of the heart in EFCC mice. Moreover, introduction of *Ews-Fli1* cDNA significantly induced apoptosis in primary cardiac myocytes, indicating the cardiac toxicity of the fusion gene. The cell type-specific epigenetic status may modulate growth inhibitory and tumorigenic activities of EWS-FLI1. Indeed, different chromatin modification was observed between Ewing's sarcoma-sensitive eSZ and –resistant eGP cells[16]. It is noted that wild-type FLI1 protein represses *Col1a1* expression, inhibiting cardiac fibrosis[22]. Interestingly, EWS-FLI1 enhanced *COL1A1* expression in human cardiac fibroblasts, suggesting that it might accelerate fibrotic processes in cardiomyopathy.

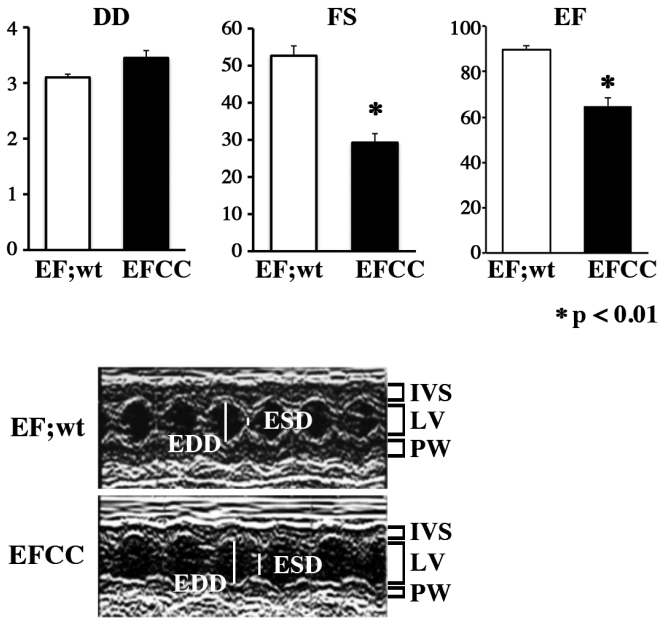

Figure 5 | Echocardiographic analysis of 37-week-old EFCC and EF;wild-type mice. Analysis of cardiovascular function (top). DD, diastolic diameter of left ventricle; FS, fractional shortening; EF, ejection fraction. Representative echocardiogram for wild-type and EFCC mice (bottom). EDD, end-diastolic diameter; ESD, end-systolic diameter, IVS, interventricular septum; LV, left ventricle; PW, posterior wall.

A number of transcription factors are associated with the development and maintenance of cardiac myocytes, and mutations in these factors affect cardiac homeostasis, structure and functions[23]. Over-expression of *E2F6* activates gene expression in myocardium and induces dilated cardiomyopathy in mice[24]. Moreover, mutations in *NKX2-5* and *PDRM16* were found associated with human congenital dilated cardiomyopathy[25,26]. It has been proposed that these proteins regulate genes involved in the ubiquitin proteasome system or proliferation of cardiomyocytes, suggesting different aspects of myocardial damage from the present model. Nevertheless, similar phenotypes shown in these models indicate the importance of cardiac-specific transcriptional regulation by transcription factors, given the low regenerative activity of adult cardiomyocytes.

Methods

Mice and gene targeting. The *Ewsr1* and *Fli1* targeting vectors were assembled in a pBSKSTKLoxPNeoGFP plasmid containing appropriate *lox*P sites, a *lox*P-flanked thymidine kinase (*Tk*) promoter-driven *neo* gene and a *Tk* promoter-driven diphtheria toxin gene. A *Gfp* gene was inserted immediately downstream of the 3′ *lox*P site for the *Ewsr1* vector. The homologous regions of the *Ewsr1* vector consisted of an 8.4 kb genomic fragment containing *Ewsr1* exons 5 to 7 and a 1.3 kb flanking exon 8 (Fig. 1a). Similarly, the *Fli1* vector included a 5.4 kb genomic fragment of *Fli1* intron 5 and a 2.0 kb fragment flanking exon 6. A CMV promoter sequence was also inserted immediately upstream of the 5′ *lox*P site of the *Fli1* vector. To establish mice carrying a single *lox*P allele of *Ewsr1* or *Fli1* genes, the linearized targeting vectors were electroporated into E14 ES cells, and drug-resistant colonies were screened for homologous recombination. To remove the *lox*P-flanked neomycin-resistant gene cassette, the pMCCreGKPuro vector was electroporated into the ES cells, and puromycin-resistant colonies were selected. Targeted clones were injected into C57BL/6 blastocysts and the resultant chimeric mice were bred to produce progeny having germ line transmission of the mutated allele. Mice harboring a targeted *Ewsr1* allele ($Ewsr1^{fl/+}$) and a targeted *Fli1* allele ($Fli1^{fl/+}$) were crossed to establish the mice that possessed *lox*P sites both in *Ewsr1* intron 7 and in *Fli1* intron 5. The resultant

Table 2 | Echocardiographic and hemodynamic analysis

	E/F; wt (n=3)	EFCC (n=4)
Echocardiographic data		
LVDd (mm)	3.01 ± 0.06	3.45 ± 0.13
LVDs (mm)	1.43 ± 0.07	2.43 ± 0.14
IVST (mm)	1.07 ± 0.03	0.78 ± 0.08
LVPWT (MM) **	1.06 ± 0.01	0.76 ± 0.04
FS (%)*	52.67 ± 2.67	29.25 ± 2.43
EF (%)*	89.67 ± 1.67	64.75 ± 3.75
Hemodynamic data		
HR (bpm)	580.7 ± 36.7	631.5 ± 11.9
sBP (mm Hg)	104.3 ± 3.8	105.5 ± 1.4
dBP (mm Hg)	57.7 ± 7.4	50.8 ± 4.5

Values are means ± SEM. LVDd, left ventricular end-diastolic dimension; LVDs, LV end-systolic dimension; IVST, interventricular septum thickness; LVPWT, left ventricular posterior wall thickness; FS, fractional shorting; EF, ejection fraction; HR, heart rate; sBP, systolic blood pressure; dBP, diastolic blood pressure; *, $p < 0.01$; **, $p < 0.05$.

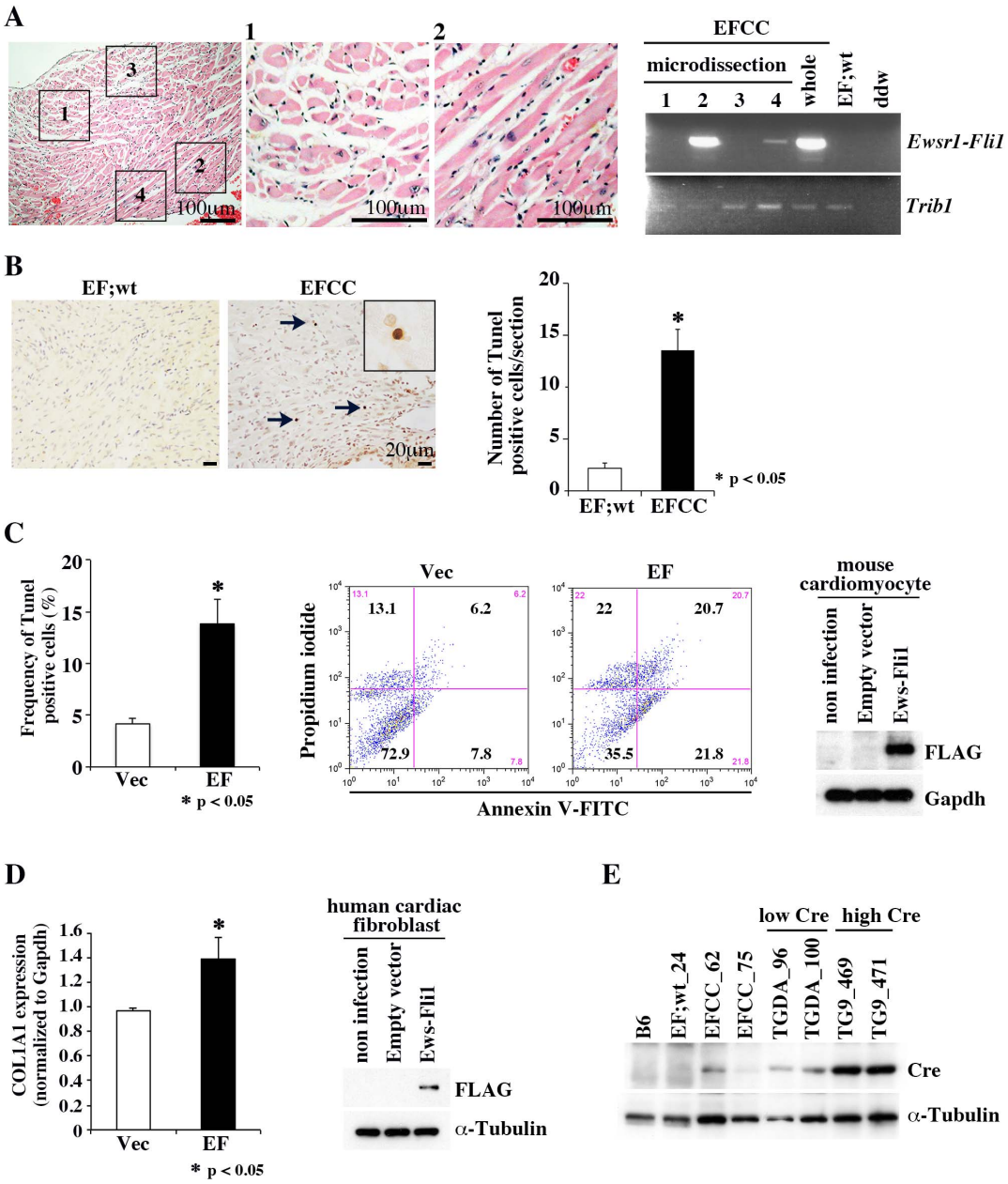

Figure 6 | The cardiac lesion in the EFCC mouse and *Ewsr1-Fli1* translocation. (A) Detection of *Ewsr1-Fli1* translocation in the myocardium. The frozen section of the cardiac tissue from the EFCC mouse was laser microdissected for the indicated areas (1-4) (left). Genomic PCR using DNA samples obtained by laser microdissection (right). (B) A TUNEL assay showed a significantly greater increase of apoptotic cell death in the myocardium of the EFCC mouse than in that of the wild-type mouse (left). High power view of the apoptotic cell is shown in the magnified inset. Frequencies of TUNEL-positive cells per section are compared between wild type and EFCC mice (right). (C) *Ewsr1-Fli1* cDNA expression induced apoptotic cell death of cardiac myocytes *in vitro*. The apoptotic cells were measured by positive signals in a TUNEL assay (left). Ewsr1-Fli1-induced cell death was further analyzed by Annexin V/PI staining and FACS analysis. The lower right quadrant (Annexin V+/PI-) represents early apoptosis, while the upper right quadrant (Annexin V+/PI+) and the upper left quadrant (Annexin V-/PI+) represent late apoptosis and necrosis, respectively. Data are representatives of three independent experiments with similar results (center). The expression of EWS-FLI1 protein in cardiac myocytes was detected by Western blotting using anti-FLAG M2 antibody (right). (D) Quantitative real-time RT-PCR for COL1A1 in human cardiac fibroblasts with or without Ewsr1-Fli1 (left). Expression of EWS-FLI1 protein was detected by Western blotting using anti-FLAG M2 antibody (right). (E) Expression of the Cre protein in the heart of EFCC mice and other *Cre* transgenic lines of variable expression levels[12].

Ewsr1$^{fl/+}$ and *Fli1*$^{fl/+}$ mice were further crossed with *CAG-Cre*, *Mx1-Cre* or *Rosa26-CreER* mice[27–29]. Genotyping of the mice was performed using primers described below. Animals were handled in accordance with the guidelines of the animal care committee at the Japanese Foundation for Cancer Research, which gave ethical approval for these studies.

Southern blotting. Southern blotting was carried out using standard procedures[30]. Genomic DNA samples were digested with *Xba*I or *Sac*I and probed with genomic DNA fragments derived from *Ewsr1* or *Fli1* loci (Fig. 1a).

Fluorescence *in situ* hybridization (FISH). The BAC clones, RPCI-23 64E17 downstream from *Ewsr1* on mouse chromosome 11 and RPCI-23 218O31 upstream from *Fli1* on chromosome 9 were purchased from Invitrogen (Carlsbad, CA) for FISH analysis. The FISH analysis using metaphase spreads obtained from embryonic fibroblasts of the *Ewsr1*$^{fl/+}$:*Fli1*$^{fl/+}$:*CAG-Cre* (EFCC) mouse was performed according to the methods previously described[31].

Genomic and reverse transcription-polymerase chain reaction (gPCR and RT-PCR). Genomic DNA (100 ng) was subjected to 35 cycles of PCR amplification. The

PCR primers to detect the *Ewsr1-Fli1* fusions were as follows. For *Ewsr1-Fli1, Ewsr1* forward primer 5′-ccccagtgcttatccttacatttg-3′ and *Fli1* reverse primer 5′-cctgacccgtgtctttgtag-3′, and for *Fli1-Ewsr1, Fli1* forward primer 5′-agagaacccactgcttactgg-3′ and Ewsr1 reverse primer 5′-accacgccctccaggttcac-3′ were used. To detect the rare translocation in *Rosa26-CreER* and *Mx1-Cre* transgenic mice, genomic DNA samples were pre-amplified using 35 cycles of PCR using the following primers. For *Ewsr1,* the 5′ primer was 5′-ccaagtaggggctctgtcag-3′ and for *Fli1,* the 3′ primer was 5′-ggagctgaagcagtaggaag-3′. For *Fli1,* the 5′ primer was 5′-gccccattgacgcaaatggg-3′ and for Ewsr1, the 3′ primer was 5′-ggggtacttggtgaaggtgc-3′. Genomic PCR for the wild-type *Ewsr1* transgene, Cre recombinase or *Trib1* was performed using the following primers: *Ewsr1,* forward, 5′-cccagtgcttatccttacatttg-3′ and GFP, reverse, 5′-accacgccctccaggttcac-3′, Cre, forward, 5′-catacctggaaaatgcttctgtcc-3′ and Cre, reverse, 5′-attgctgtcacttggtcgtggc-3′, or *Trib1,* forward, 5′-cagtctctccttccaagtcatc-3′ and *Trib1*, reverse, 5′-gattgttgctgctgttgttc-3′. The PCR products were analyzed by 2% agarose gel electrophoresis.

RT-PCR was carried out using cDNA generated from total RNA of systemic organs as previously described[32]. The *Ewsr1-Fli1* fusion transcript was amplified using *Ewsr1* exon 7 primer (5′-tcctcttcacagccgac-3′) and *Fli1* exon 6 primer (5′-ctgctcagtgttcttgcc-3′). The primers for Cre recombinase (forward, 5′-cggtctggcagtaaaaactat-3′; reverse, 5′-cagggtgttataagcaatccc-3′) and *Hprt* (forward, 5′-gctggtgaaaaggacctct-3′; reverse, 5′-cacaggactagaacacctgc-3′) were also used. The PCR products were purified, sub-cloned into a plasmid and sequenced. Real-time quantitative RT-PCR was performed by using a Fast Real-Time PCR System (Applied Biosystems, Foster City, CA). The primers for human *COL1A1* (forward, 5′-catgaccgagacgtgtggaa-3′; reverse, 5′-tttcttggtcggtgggtgac-3′) and GAPDH (forward, 5′-acctgacctgccgtctagaa-3′; reverse, 5′-aaagtggtcgttgagggcaa-3′) were used.

Echocardiography. Transthoracic echocardiography was performed on conscious, gently restrained mice using a 15-MHz linear probe (Power-Vision 8000, Toshiba, Tokyo, Japan), as described previously[33]. Parasternal long-axis view and short axis view of the left ventricle at the level of the papillary muscles were obtained. 2D-guided M-mode recordings were obtained from short axis view at the level of the papillary muscles. Measurements of interventricular septum thickness (IVST) and left ventricular posterior wall thickness (LVPWT) were made from M-mode recordings in diastole. Left ventricular internal diameter at end-diastole (LVDd) and end-systole (LVDs) were measured from M-mode recordings. Fractional shortening (FS) was calculated as $100 \times [(\mathrm{LVDd} - \mathrm{LVDs})/\mathrm{LVDd}]$ (%). Ejection fraction (EF) was calculated using the Teichholtz method.

Cell culture and recombinant lentivirus infection. Primary neonatal ICR mouse ventricular myocytes were purchased from Cosmo Bio (Tokyo, Japan), and cells were cultured with D-MEM/F-12 medium supplemented 10% fetal bovine serum (HyClone, South Logan, UT). Human cardiac fibroblasts were purchased from PromoCell (Heidelberg, Germany), and cells were cultured with Fibroblast Medium (ScienCell, Carlsbad, CA). The human *EWSR1-FLI1* cDNA (a kind gift from Susanne Baker) was FLAG-tagged and inserted into the pLVSIN-CMV-neo plasmid (Takara Bio, Tokyo, Japan) and HEK 293 cells were transfected with the plasmid using Lipofectamine 2000 (Invitrogen). Cells were harvested 48 h after lentiviral infection and subjected to further analyses.

TUNEL assay and Annexin-V analysis. Formaldehyde-fixed and paraffin-embedded cardiac tissue sections or methanol-fixed murine primary cardiac myocytes were subjected to TUNEL assays using the DeadEnd Colorimetric TUNEL System (Promega, Madison, WI) according to the manufacturer's protocol. For the Annexin V analysis cells were stained with Annexin V-FITC and propidium iodide (PI) according to the manufacturer's instruction (BD Bioscience Pharmingen, San Diego, CA). The stained cells were immediately evaluated using a FACSCalibur flow cytometer (BD Biosciences, Franklin Lakes, NJ).

Western blotting. Western blotting was performed as previously described[32]. A monoclonal anti-FLAG M2 antibody was purchased from Sigma (St Louis, MO), anti-Cre from Chemicon (Temecula, CA), anti-α-tubulin from Sigma and anti-GAPDH from HyTest (Turku, Finland).

Statistical analysis. Results are shown as means ± standard errors of the mean (SEM). Continuous distributions were compared with two-tailed Student's *t*-tests. Survival analysis was performed using the Kaplan-Meier life table method, and the survival between groups was compared with the log-rank test. All *P* values were two-sided, and a *P* value of less than 0.05 was considered significant.

1. Mitelman, F., Johansson, B. & Mertens, F. The impact of translocation and gene fusions on cancer causation. *Nat. Rev. Cancer* **7**, 233–245 (2007).
2. Taylor, B. S. *et al.* Advances in sarcoma genomics and new therapeutic targets. *Nat. Rev. Cancer* **11**, 541–557 (2011).
3. Smith, A. J. H. *et al.* A site-directed chromosomal translocation induced in embryonic stem cells by Cre-*lox*P recombination. *Nat. Genet.* **9**, 376–385 (1995).
4. Van Deursen, J., Fornerod, M., van Rees, B. & Grosveld, G. Cre-mediated site-specific translocation between nonhomologous mouse chromosomes. *Proc. Natl. Acad. Sci. USA* **92**, 7376–7380 (1995).
5. Forster, A. *et al.* Engineering de novo reciprocal chromosomal translocations associated with *Mll* to replicate primary events of human cancer. *Cancer Cell* **3**, 449–458 (2003).
6. Delattre, O. *et al.* Gene fusion with an *ETS* DNA-binding domain caused by chromosome translocation in human tumours. *Nature* **359**, 162–165 (1992).
7. Sorensen, P. H. *et al.* A second Ewing's sarcoma translocation, t(21;22), fuses the EWS gene to another ETS-family transcription factor, ERG. *Nat. Genet.* **6**, 146–151 (1994).
8. Ordonez, J. L., Osuna, D., Herrero, D., de Alava, E. & Madoz-Gurpide, J. Advances in Ewing's sarcoma research: where are we now and what lies ahead? *Cancer Res.* **69**, 7140–7150 (2009).
9. Torchia, E. C., Boyd, K., Rehg, J. E., Qu, C. & Baker, S. J. *EWS/FLI-1* induces rapid onset of myeloid/erythroid leukemia in mice. *Mol. Cell. Biol.* **27**, 7918–7934 (2007).
10. Zucman, J. *et al.* Combinatorial generation of variable fusion proteins in the Ewing family of tumours. *EMBO J.* **12**, 4481–4487 (1993).
11. Riggi, N., Cironi, L., Suva, M. L. & Stamenkovic, I. Sarcomas: genetics, signaling, and cellular origins. Part I: The fellowship of TET. *J. Pathol.* **213**, 4–20 (2007).
12. Buerger, A. *et al.* Dilated cardiomyopathy resulting from high-level myocardial expression of Cre-recombinase. *J. Card. Fail.* **12**, 392–398 (2006).
13. Collins, E. C., Pannell, R., Simpson, E. M., Forster, A. & Rabbitts, T. H. Inter-chromosomal recombination of *Mll* and *Af9* genes mediated by cre-*loxP* in mouse development. *EMBO Rep.* **1**, 127–132 (2000).
14. Drynan, L. F. *et al. Mll* fusions generated by Cre-*loxP*-mediated *de novo* translocations can induce lineage reasignment in tumorigenesis. *EMBO J.* **24**, 3136–3146 (2005).
15. Buchholz, F., Regaeli, Y., Trumpp, A. & Bishop, J. M. Inducible chromosomal translocation of *AML1* and *ETO* genes through Cre/loxP-mediated recombination in the mouse. *EMBO Rep.* **11**, 133–139 (2000).
16. Tanaka, M. *et al.* Ewing's sarcoma precursors are highly enriched in embryonic osteochondrogenic progenitors. *J. Clin. Invest.* **121**, 3061–3074 (2014).
17. Storm, E. E. & Kingsley, D. M. GDF5 coordinates bone and joint formation during digit development. *Dev. Biol.* **209**, 11–27 (1999).
18. Vijayaraj, P. *et al.* Erg is a crucial regulator of endocardial-mesenchymal transformation during cardiac valve morphogenesis. *Development* **139**, 3973–3985 (2012).
19. Deneen, B. & Denny, C. T. Loss of p16 pathways stabilizes EWS/FLI1 expression and complements EWS/FLI1 mediated transformation. *Oncogene* **20**, 6731–6741 (2001).
20. Lessnick, S. L., Dacwag, C. S. & Golub, T. R. The Ewing's sarcoma oncoprotein EWS/FLI induces a p53-dependent growth arrest in primary human fibroblasts. *Cancer Cell* **1**, 393–401 (2002).
21. Sohn, E. J. *et al.* EWS/FLI1 oncogene activates caspase 3 transcription and triggers apoptosis *in vivo*. *Cancer Res.* **70**, 1154–1163 (2010).
22. Elkareh, J. *et al.* Marinobufagenin induces increases in procollagen expression in a process involving protein kinase C and Fli-1: implications for uremic cardiomyopathy. *Am. J. Physiol. Renal. Physiol.* **296**, F1219–F1226 (2009).
23. Oka, T., Xu, J. & Molkentin, J. D. Re-employment of developmental transcription factors in adult heart disease. *Semin. Cell Dev. Biol.* **18**, 117–131 (2007).
24. Westendorp, B. *et al.* The E2F6 repressor activates gene expression in myocardium resulting in dilated cardiomyopathy. *FASEB J.* **26**, 2569–2579 (2012).
25. Costa, M. W. *et al.* Functional characterization of a novel mutation in *NKX2-5* associated with congenital heart disease and adult-onset cardiomyopathy. *Circ. Cardiovasc. Genet.* **6**, 238–247 (2013).
26. Arndt, A. K. *et al.* Fine mapping of the 1p36 deletion syndrome identifies mutation of *PRDM16* as a cause of cardiomyopathy. *Am. J. Hum. Genet.* **93**, 67–77 (2013).
27. Sakai, K. & Miyasaki, J. A transgenic mouse line that retains Cre recombinase activity in mature oocytes irrespective of the cre transgene transmission. *Biochem. Biophys. Res. Commun.* **237**, 318–324 (1997).
28. Kuhn, R., Schwenk, F., Aguet, M. & Rajewsky, K. Inducible gene targeting in mice. *Science* **269**, 1427–1429 (1995).
29. Ventura, A. *et al.* Restoration of p53 function leads to tumour regression *in vivo*. *Nature* **445**, 661–665 (2007).
30. Iwasaki, M. *et al.* Identification of cooperative genes for NUP98-HOXA9 in myeloid leukemogenesis using a mouse model. *Blood* **105**, 784–793 (2005).
31. Kawamura-Saito, M. *et al.* Fusion between CIC and DUX4 up-regulates PEA3 family genes in Ewing-like sarcomas with t(4;19)(q35;q13) translocation. *Hum. Mol. Genet.* **15**, 2125–2137 (2006).
32. Nakamura, T. *et al.* Evi9 encodes a novel zinc finger protein that interacts with BCL6, a known human B-cell proto-oncogene. *Mol. Cell. Biol.* **20**, 3178–3186 (2009).
33. Kuwahara, K. *et al.* NRSF regulates the fetal cardiac gene program and maintains normal cardiac structure and function. *EMBO J.* **22**, 6310–6321 (2003).

Acknowledgments

We are grateful to Junichi Miyazaki for CAG-Cre, Klaus Rajewsky for MX1-Cre and Tyler Jacks for Rosa26-Cre transgenic mice. We also thank Miki Yamazaki, Yohei Kanno, Hitomi Yamanaka and Tokuichi Kawaguchi for technical assistance. This work was supported by

the Grants-in-Aid for Scientific Research from the Ministry of Education, Culture, Sports, Science and Technology (23791672 and 26250029) to M.T. and T.Na.

Author contributions

M.T., T.No. and T.Na. designed the work. M.T., S.Y., Y.Y. and H.K. performed the experiments. M.T., K.K., K.N., P.Y.J., T.No. and T.Na. analyzed the data. M.T. and T.Na. wrote the paper. All co-authors contributed in the form of discussion and critical comments.

Additional information

Competing financial interests: The authors declare no competing financial interests.

How to cite this article: Tanaka, M. *et al*. Somatic chromosomal translocation between *Ewsr1* and *Fli1* loci leads to dilated cardiomyopathy in a mouse model. *Sci. Rep.* **5**, 7826; DOI:10.1038/srep07826 (2015).